JOURNAL OF VIROLOGY, Feb. 1990, p. 731–741
0022-538X/90/020731-11$02.00/0

Vol. 64, No. 2

# Neutralization-Resistant Variants of a Neurotropic Coronavirus Are Generated by Deletions within the Amino-Terminal Half of the Spike Glycoprotein†

THOMAS M. GALLAGHER, SUEZANNE E. PARKER, AND MICHAEL J. BUCHMEIER*
*Department of Immunology, Scripps Clinic and Research Foundation, La Jolla, California 92037*

Received 14 June 1989/Accepted 13 October 1989

**Neuroattenuated variants of mouse hepatitis virus type 4 (MHV-4) selected for resistance to neutralizing monoclonal antibodies (R. G. Dalziel, P. W. Lampert, P. J. Talbot, and M. J. Buchmeier, J. Virol. 59:463–471, 1986) were found to harbor large deletions in both mRNA 3 and its protein product, the 180-kilodalton virion spike (S) glycoprotein. By using antipeptide antibodies directed against selected portions of the chain, deletions were mapped to the middle of the amino-terminal S1 fragment, one of the two posttranslational cleavage products of S, and involved omission of 15 kilodaltons of protein. Deletion mutants could be selected only after multiple passage of virus through cultured cell lines; minimally passaged MHV-4 stocks contained putative point mutants selectable by neutralizing monoclonal antibodies but no deletions. Enhanced growth of deletion mutants relative to wild-type virus was observed in four cell lines used for virus propagation and was attributed to delayed and diminished cytopathic effects that allowed cultures to support virus production for prolonged periods. This hypothesis was reinforced by the finding that no selective advantage for the deletion mutants was observed in two cell lines resistant to virus-induced cytopathic effects. These results indicate that the passaging of MHV-4 in culture generates heterogeneity in S structure and eventually selects for rare neutralization-resistant deletion mutants with decreased virulence properties.**

Mouse hepatitis virus type 4 (MHV-4; strain JHM) is a neurotropic member of the family *Coronaviridae*. Intracerebral inoculation of mice with this virus typically results in a rapidly fatal encephalomyelitis (1). Variants of MHV-4, however, have been generated by chemical mutagenesis (11), growth in persistently infected cell culture (2, 12), and multiple passage in mouse brain (31). The resulting variants, selected for temperature sensitivity (11) or small-plaque morphology (31), were often found to be attenuated in murine hosts. In most cases, infection with these mutants leads to a chronic sublethal demyelinating disease without encephalitis (11, 16).

The correlation of genetic lesions on these variants with neuroattenuation has been hampered by selection methods that did not restrict the range of mutations to a single viral gene. However, multiple libraries of neutralizing monoclonal antibodies directed against the 180-kilodalton (kDa) spike glycoprotein (S; formerly termed E2) of MHV-4 have been prepared (8, 38, 39), and these have served as selecting agents in the isolation of naturally occurring neutralization-resistant variants. Three separate studies addressing the selection and relative pathogenicity of these neutralization-resistant variants have shown that they possess a neuroattenuation phenotype similar to that seen with previously isolated variants (7, 9, 40).

Although these studies showed that at least one determinant associated with neurovirulence of MHV-4 was present on S, they did not further define its location within the protein. Accumulated facts pertaining to the structure of coronavirions did, however, provide clues as to its position. S is known to comprise the characteristic spikes projecting 20 nm from the virion envelope. These spikes, which are thought to be dimers or trimers of S (5), serve as ligands in virus-cell receptor binding (6, 33) and when expressed on the cell surface have fusogenic activity that results in syncytium formation and recruitment of cells into the infection cycle (6, 10). In contrast to S, the virion matrix glycoprotein M is largely embedded within the membrane, and phosphoprotein N (nucleocapsid) remains associated with the internal 26-kilobase RNA genome (33). The 180-kDa S chain is cleaved posttranslationally into two 90-kDa fragments termed S1 and S2, previously termed 90B (S1) and 90A (S2) (34). Both biochemical and amino acid sequence information has suggested that the carboxy-terminal S2 fragment is an integral membrane protein that comprises the stalk portion of the spikes, whereas the amino-terminal S1 is a peripheral fragment that likely makes up the apices of the peplomers (29). S is the most polymorphic of the three virion proteins (37), and comparative analyses of the known amino acid sequences of S from MHV strains A59 (21) and JHM (28) have shown that this heterogeneity is heavily represented in S1. In addition, the sequence comparison revealed 89 amino acid residues within S1 that were unique to strain A59. Thus, because of its surface exposure and relative polymorphism, fragment S1 seemed the most likely site for the various neutralizing epitopes correlated with neurovirulence.

Here we report on the genotype and phenotype of neutralization-resistant and neuroattenuated variants of MHV-4. We have found that these variants are indeed altered in the S1 posttranslational fragment. They comprise a class of deletion mutants of wild-type MHV-4 that lack an estimated 150 amino acids from the middle of S1. These mutants were found at high frequencies only in in vitro-passaged stocks of MHV-4 and possessed reduced in vitro cytotoxicity which we propose is a result of a lower capacity of the deletion mutants to fuse susceptible cells.

* Corresponding author.
† Publication no. 5932-IMM from the Department of Immunology, Scripps Clinic and Research Foundation.

## MATERIALS AND METHODS

**Cells.** Six murine cell lines were used in this study; Sac- (rhabdomyosarcoma), DBT (astrocytoma), C1300, Neuro 2A (two peripheral neuroblastomas), and OBL 21 and OBL 21A (two central nervous system-derived neuronal cultures). Sac- and DBT cells were obtained from M. M. C. Lai (University of Southern California, Los Angeles). C1300 and Neuro 2A cells were obtained from the American Type Culture Collection, Rockville, Md. OBL 21 and OBL 21A cells were a gift of C. Cepko (Harvard University, Cambridge, Mass.). All cell lines were grown as adherent monolayer cultures at 37°C. Growth medium was Dulbecco minimal essential medium supplemented with either 8% calf serum for DBT and Sac- cells or 10% fetal calf serum for C1300, Neuro 2A, OBL 21, and OBL 21A cells.

**Viruses and infection.** Two strains of MHV were used: MHV-4, originally obtained from L. Weiner (41), and MHV A59, which was obtained from the American Type Culture Collection. All stocks used represented the progeny from a single plaque. Infections of cell cultures with these viruses were performed as described previously for infection of Sac- cells with MHV A59 (33). Briefly, virus was absorbed to 90% confluent monolayers for 1 h at 37°C in growth medium. Unattached inoculum was then removed and replaced with fresh growth medium, and progress of infection was monitored by examination of syncytium development. At the indicated times after inoculation, virus-containing extracts were prepared by three freeze-thaw cycles (−70 to +20°C). Debris was then removed by low-speed centrifugation (5,000 × *g* for 15 min at 5°C), and the resulting clarified extracts were stored at −70°C. Infectivity in the extracts was determined by plaque titration on DBT cells. Where indicated, passaged stocks of MHV-4 were subjected to an additional three cycles of plaque purification on DBT cells, and virus from the final well-isolated plaque was amplified in Sac- cells as described above to generate a fresh working virus stock.

**Selection of MAb-resistant variants.** The monoclonal antibodies (MAbs) used were generated in this laboratory (6), and their properties have been described elsewhere (38). Original (1986) MAb-resistant variants were selected as described previously (7), and newly selected (1989) variants were obtained similarly, with minor modifications. In brief, 1-ml stocks of MHV-4 containing $10^6$ PFU were mixed with an equal volume of MAb ascites fluid diluted 10-fold in growth medium and incubated for 1 h at 22°C. The virus-MAb mixture was then used to inoculate DBT cell monolayers. After 1 h at 37°C, inoculum was removed and replaced with medium containing a 1:50 dilution of ascites fluid. After 24 h, the foci of infection, which often occupied extremely small areas involving only 10 to 20 cells, were pooled into a single clarified freeze-thaw extract and subjected to two additional rounds of neutralization and amplification as described above. The resulting neutralization-resistant virus populations were stored at −70°C as clarified extracts. Variants are designated according to the selecting MAb used (MAb 5A13.5 or 4B11.6) and the year of isolation (1986 [86] or 1989 [89]). Plaque-purified isolates from the 1986 selections are indicated by clone numbers (i.e., V5A13.1, -.2, -.3, etc.). Variants known to have deletions are designated by Δ; those without a Δ are candidate point mutants.

**Infection of mice.** BALB/c Byj mice were obtained from the Scripps Clinic breeding facility at 6 weeks of age and inoculated intracerebrally with virus (1,000 PFU) in a volume of 0.05 ml of phosphate-buffered saline. At various times after infection, brains were aseptically removed, weighed, and immediately homogenized in phosphate-buffered saline, using a dispersing tool spinning at 10,000 rpm for 30 s. Infectious virus in the resulting 10% (wt/vol) brain suspensions was titrated on DBT cell monolayers, and plaques were counted 3 days later.

**Northern (RNA) blot analysis.** Total cytoplasmic RNA from infected Sac- cell monolayers was harvested after 80% of cells were involved in syncytia. At this time, cell monolayers were rinsed twice with 0.85 M NaCl and then suspended in TNE (10 mM Tris hydrochloride [pH 7.0], 100 mM NaCl, 1 mM EDTA) containing 0.5% Nonidet P-40 (NP-40), to $10^6$ cells per ml. After vigorous pipetting to homogenize the lysates, nuclei were immediately pelleted (14,000 × *g* for 2 min), and cytoplasmic supernatants were mixed with an equal volume of TNE-saturated phenol. After two extractions with phenol and one with chloroform, RNA was ethanol precipitated, suspended in water, and quantitated spectrophotometrically.

Electrophoresis of RNA was performed as described previously (24) in 1.5% agarose gels containing MOPS buffer (20 mM morpholinepropanesulfonic acid, 5 mM sodium acetate, 0.1 mM EDTA [pH 7.0]) and 2.2 M formaldehyde. RNA samples (5 μg) were denatured in 50% formamide and 2.2 M formaldehyde by heating to 68°C for 5 min and then electrophoresed at 1.2 V/cm for 16 h with recirculation of the MOPS running buffer. After electrophoresis, the gel was rinsed with water and then with 50 mM NaOH to partially hydrolyze RNAs, after which it was equilibrated with 20× SSC (1× SSC is 0.15 M NaCl plus 0.015 M sodium citrate). RNAs were transferred to nitrocellulose filters (0.45 μm pore size; Schleicher & Schuell, Inc.) by capillary diffusion and baked at 80°C under vacuum.

For hybridization probes, we used a cDNA clone (a gift of W. Spaan, University of Utrecht, Utrecht, Netherlands) that consisted of a *Hpa*II fragment representing nucleotides 636 to 840 of the MHV A59 nucleocapsid gene (RNA 7) provided within vector SP65. To prepare an RNA probe, portions of this plasmid were cleaved with *Hin*dIII, and 0.5-μg samples of the linearized template were used in runoff in vitro transcription reactions to generate minus-strand RNA 7 sequences. Reactions were performed according to standard procedures (25), using SP6 RNA polymerase (Promega Biotec). RNAs were radiolabeled by addition of 50 μCi of [α-$^{32}$P]UTP (Amersham Corp.) to each 20-μl reaction volume. Yields of about 5 to 10 μg of RNA containing $10^8$ $^{32}$P dpm were typically obtained.

Nitrocellulose filters were prehybridized at 65°C for 3 h in 50% deionized formamide–5× SSC–2× Denhardt solution–150 μg of sonicated salmon sperm DNA per ml–0.1% sodium dodecyl sulfate (SDS). Hybridizations were performed in the same solution at 65°C for 18 h with $10^6$ dpm of [$^{32}$P]RNA per ml. Filters were washed at 37°C in 2× SSC–0.1% SDS and then at 37°C in 0.1× SSC–0.1% SDS, air dried, and exposed to Kodak XAR-5 film.

**Pulse-labeling and radioimmunoprecipitation of virus-specific proteins.** Infected monolayers ($10^5$ cells per cm$^2$) were radiolabeled when 50 to 100% syncytia was observed but before cell detachment. Medium was carefully removed from each culture well, cells were rinsed twice with 0.85 M NaCl, and methionine-deficient Dulbecco modified Eagle medium containing 4% calf serum and 100 μCi of [$^{35}$S]methionine (Amersham) per ml was added. After 1 h at 37°C, the labeling medium was removed, and cells were again rinsed twice with 0.85 M NaCl to remove unincorporated methionine. Cytosol extracts were prepared by solubilizing the cells to 5 × $10^6$/ml in lysis buffer (TNE containing

0.5% NP-40, 0.3 trypsin inhibitor units of aprotinin per ml, and 1 mM phenylmethylsulfonyl fluoride) and by subsequent clarification by centrifugation (14,000 × *g* for 2 min).

S was immunoprecipitated from the extracts with rabbit antiserum (kindly provided by K. Holmes, Uniformed Health Services, Bethesda, Md.) and staphylococcal protein A (15). Samples (0.1 ml) were preabsorbed with 0.01 ml of a 10% (vol/vol) suspension of Pansorbin (Calbiochem-Behring) in lysis buffer, clarified, and incubated with 0.001 ml of antiserum for 1 h at 22°C. A 0.025-ml amount of 10% Pansorbin was added; 15 min later, the immune complexes were pelleted (14,000 × *g* for 1 min) and washed once with Tris (0.01 M Tris hydrochloride [pH 7.2]) containing 1 M NaCl and 0.1% NP-40, once with Tris–0.1 M NaCl–0.001 M EDTA–0.1% NP-40–0.3% SDS, and once with Tris–0.1% NP-40. The final pellet was mixed with 0.1 ml of solubilizing solution (0.062 M Tris hydrochloride [pH 6.8], 2% SDS, 5% 2-mercaptoethanol, 2.5% Ficoll [Pharmacia Fine Chemicals]) and heated for 5 min at 100°C. Samples (0.02 ml, corresponding to $10^5$ cells) were electrophoresed on Laemmli slab gels containing 3% (wt/vol) and 8% (wt/vol) acrylamide in the stacking and resolving gel components, respectively. After electrophoresis (10 V/cm for 5 h), gels were soaked for 2 h in 10% acetic acid–25% methanol, vacuum dried, and exposed for 2 days to Kodak XAR-5 film.

**Antipeptide antibodies.** Three antipeptide antibodies were used. Each was directed against peptides derived from the sequence of the S protein of MHV A59. These were peptide A (CAQPDIVSPC; S amino acids 481 to 490), peptide B (CVDYSKSRRAHR; amino acids 706 to 717), and peptide C (SVSTGYRLTTC; amino acids 718 to 727). Peptides were synthesized, purified, linked to keyhole limpet hemocyanin, and used to immunize rabbits by previously described procedures (3). Anti-A and anti-C sera were used for Western blotting (immunoblotting) at 1:100 dilutions; anti-B serum was used at 1:500. For all antisera, specificity was demonstrated by blocking reactivity against S with free peptide as described elsewhere (3).

**Western blot analysis.** Samples for Western blot analysis were prepared by concentrating virions from clarified infected-cell lysates. Lysates (10 ml) were underlaid successively with 9-ml volumes of 10, 20, and 30% (wt/wt) sucrose solutions in HNE buffer (0.05 M sodium *N*-2-hydroxyethylpiperazine-*N'*-2-ethanesulfonic acid [HEPES; pH 7.0], 0.1 M NaCl, 0.001 M EDTA) containing 0.01% bovine serum albumin, and then virions were pelleted through the sucrose solutions by using a Beckman Spinco SW28 rotor (25,000 rpm for 5 h at 5°C). Pellets were resuspended in 0.5 ml of ice-cold HNE buffer and stored at −70°C.

For electrophoresis, 0.01- to 0.02-ml samples of each resuspended pellet were mixed with an equal volume of 2× solubilizing solution and heated to 100°C for 5 min. Electrophoresis was in continuous slab gels containing 7.5% (wt/vol) acrylamide, 0.1 M Tris base, 0.1 M bicine (*N*,*N*-bis[2-hydroxyethyl] glycine), and 0.1% SDS (14) at 10 V/cm for 6 h without recirculation of the 0.01 M Tris base–0.01 M bicine–0.1% SDS running buffer. Unlike the discontinuous Laemmli gels, Tris-bicine gels permitted the penetration of high-molecular-weight oligomers of S into the resolving matrix. After electrophoresis, proteins were transferred electrophoretically as described previously (4) onto 0.2-μm-pore-size nitrocellulose filters (Schleicher & Schuell) for 2 h at 1 A with continuous cooling of the transfer buffer (0.025 M Tris base, 0.2 M glycine, 20% methanol). Rainbow markers (Amersham) were used to monitor both Tris-bicine gel resolution and efficiency of protein transfer to nitrocellulose.

After transfer, the filters were preblocked overnight at 4°C in blotting buffer (phosphate-buffered saline containing 0.05% Tween 20 and 2% skimmed milk powder) (13) and then incubated with the indicated dilutions of antipeptide antiserum in the same buffer for 4 h at 22°C. Unreacted antibody was removed by successive washes with blotting buffer, and bound immunoglobulin was detected with $^{125}$I-labeled *Staphylococcus aureus* protein A (2 × $10^6$ cpm/ml in blotting buffer). Excess radioactivity was removed by extensive washes with phosphate-buffered saline containing 0.05% Tween 20; filters were then air dried and exposed to Kodak XAR-5 film with Dupont Cronex Lightning-Plus intensification screens at −70°C.

**Measurement of viral RNA synthesis by [$^3$H]uridine incorporation.** Medium from 1-cm$^2$ wells containing $10^5$ infected DBT cells was carefully removed at the indicated times and replaced with fresh medium containing 5 μg of dactinomycin (Calbiochem-Behring) per ml. After 30 min at 37°C, supernatants were replaced with labeling medium containing 5 μg of dactinomycin and 10 μCi of 5,6-[$^3$H]uridine (Amersham) per ml. After an additional 30 min at 37°C, labeling medium was removed, and lysates ($10^6$ cells per ml) were immediately prepared by addition of TNE containing 1% NP-40. Duplicate 0.025-ml samples were spotted onto Whatman GF/C filters, which were then air dried before successive washes in 20% (wt/wt) trichloroacetic acid, 8% trichloroacetic acid, 95% ethanol, and diethyl ether. Radioactivity was measured by liquid scintillation spectroscopy.

## RESULTS

**Identification of neutralization-resistant variants of MHV-4 with deletions in RNA 3, the S gene.** Previous studies have shown that different isolates of MHV often show a marked size heterogeneity in the S gene (21, 26, 35, 36). Therefore, initial experiments were designed to compare the relative sizes of our wild-type and variant mRNAs by agarose gel electrophoresis. Since this method is known to clearly distinguish 5% variations in RNA size (19), we anticipated that differences of greater than 400 bases could be identified in the 8.3-kilobase mRNA 3. To this end, total cytoplasmic RNAs from cells infected with either MHV-4, MHV A59, or two representative MAb-selected variants were subjected to electrophoresis in denaturing gels and detected by hybridization with radiolabeled RNA specific for the common 3'-end nucleocapsid gene sequences found in all seven MHV mRNAs. This analysis revealed that both independently selected variants, V4B11.3Δ(86) and V5A13.1Δ(86), contained significant deletions of about 400 bases in the S gene (Fig. 1). As predicted from the 3'-coterminal nested-set arrangement of coronavirus mRNAs, the deletion was reflected only in RNAs larger than RNA 4, although it was not readily resolved in the very large genomic-size mRNA 1.

**Localization of two distinct S deletions to sequences within the middle of the amino-terminal S1 fragment.** To demonstrate that deletion mutations in the S gene were reflected at the protein level, Sac- cell cultures were infected separately with MHV-4, MHV A59, and the various MAb-selected variants and then pulse-labeled from 11 to 12 h postinfection with [$^{35}$S]methionine. Cell-associated S was then immunoprecipitated with anti-S rabbit serum and subjected to electrophoresis.

The resulting autoradiogram (Fig. 2) illustrates the relative

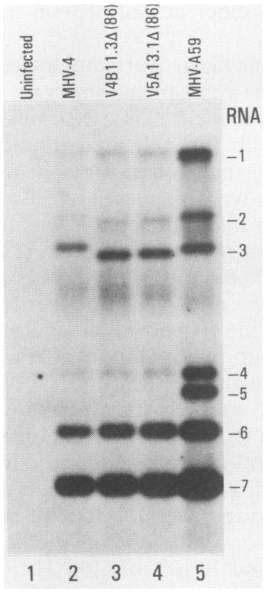


FIG. 1. Electrophoretic comparison of virus-specific RNAs from Sac- cultures infected with MHV-4, MHV A59, and original neutralization-resistant variants. Cell monolayers were inoculated with the indicated viruses and incubated at 37°C until 14 h postinfection; then cytoplasmic extracts were prepared, and RNA was isolated by phenol-chloroform extraction. RNAs (5 μg per lane) were denatured, subjected to gel electrophoresis, and transferred to nitrocellulose. Virus-specific RNAs were visualized by autoradiography after hybridization with a $^{32}$P-labeled transcript complementary to 213 nucleotides of MHV A59 mRNA 7. Recognition of MHV-4 and variant-specific RNAs by this probe is due to extensive homology between the RNA 7 segments of MHV-4 and MHV A59.

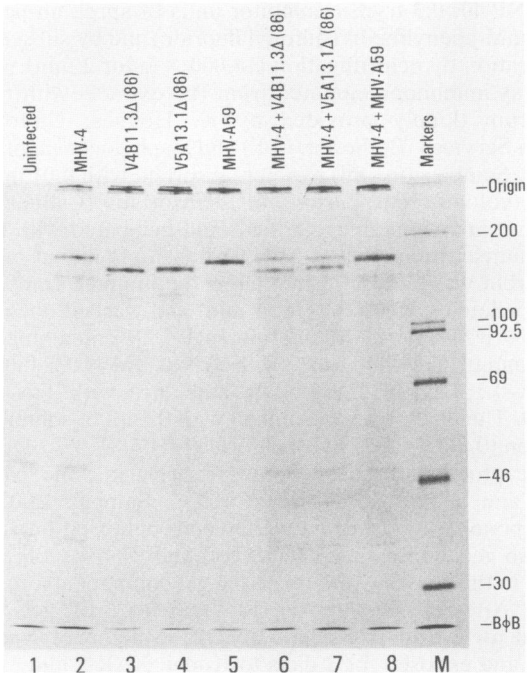


FIG. 2. Relative electrophoretic mobilities of S (180-kDa) chains synthesized in cultures infected with MHV-4, deletion variants, and MHV A59. Infected Sac- cell monolayers were radiolabeled with [$^{35}$S]methionine from 11 to 12 h postinfection. Immediately after labeling, cell sheets were dissolved, and S molecules were immunoprecipitated from the cytoplasmic extracts with rabbit antiserum directed against S. The resulting precipitates were electrophoresed in discontinuous slab gels as described in Materials and Methods and detected by autoradiography.

sizes of the various S proteins. Variants V4B11.3Δ(86) and V5A13.1Δ(86), which previously were scored as deletion mutants in Northern blot analyses, synthesized S chains estimated to be 15 and 12 kDa, respectively, smaller than wild-type S (Fig. 2, lanes 2 to 4 and lanes 6 and 7). Both mutants synthesized S polypeptides 16 kDa smaller than wild-type virus when radiolabeling was done in the presence of the glycosylation inhibitor tunicamycin (data not shown), indicating that about 150 amino acids were deleted and that the small differences in mobility between the two mutant chains (15 versus 12 kDa smaller than wild-type S) resulted from differences in the extent of glycosylation. In addition, the migration of S from MHV-4 was slightly less than that from MHV A59 (Fig. 2; compare lanes 2, 5, and 8). This observation, in conjunction with previous sequence information on S from MHV A59 and JHM (21, 28), indicated that the order of S size on these strains is MHV-4 > MHV A59 > MHV JHM.

To localize these deletions to a specific region of S, we took advantage of the fact that S-polypeptide sequences have been deduced from the nucleotide sequences of both MHV A59 (21) and MHV JHM (28). Using this information as well as the location of the proteolytic cleavage site of S, we synthesized peptides corresponding to three regions of the chain (Fig. 3). Peptide A, which corresponds to residues near the middle of the MHV A59 S1 fragment, is not represented in MHV JHM S and thus represents a region of polymorphism between the two viruses. Peptides B and C represent the MHV A59 sequences flanking the arginine-rich S1-S2 cleavage site. After proteolysis, peptide B and C sequences reside on amino-terminal S1 and carboxy-terminal S2 fragments, respectively.

We anticipated that rabbit antisera raised against these three peptides would prove useful in the localization of S deletions in MHV-4 to fragment S1 or S2. Therefore, virion proteins from MHV strains and variants were tested for reactivity with the anti-peptide A, B, and C antisera by Western blot analysis. Anti-A serum (Fig. 3A) reacted with the S1 chains of MHV-4 and MHV A59 but not with the variants V4B11.3Δ(86) and V5A13.1Δ(86). Strong binding to a previously unidentified band specific to MHV-4 at 75 kDa (designated p75) was also observed; this protein may represent an alternate S cleavage product. The signal at the position of nucleocapsid (N) was not specific, as judged by a failure to block this binding by prior saturation of antiserum with free peptide A (data not shown). Anti-B serum reacted with the S1 proteins of all four viruses; with the exception of the bands for V5A13.1Δ(86) and MHV A59, each S1 band had a characteristic electrophoretic mobility. Anti-C serum, which reacted strongly in the analysis, identified two major bands at about 90 and 270 kDa. These bands, which coelectrophoresed in all MHV strains and variants, likely represent monomers (90 kDa) and trimers (270 kDa) of S2. Together, these results indicate that the major deletions in our MAb-resistant variants are located on fragment S1 and include a region that has been previously shown to be absent in MHV JHM.

**Reselection of neutralization-resistant variants of MHV-4 yields both point and deletion mutants.** Additional analyses of viral RNA and protein electropherotypes revealed that all of

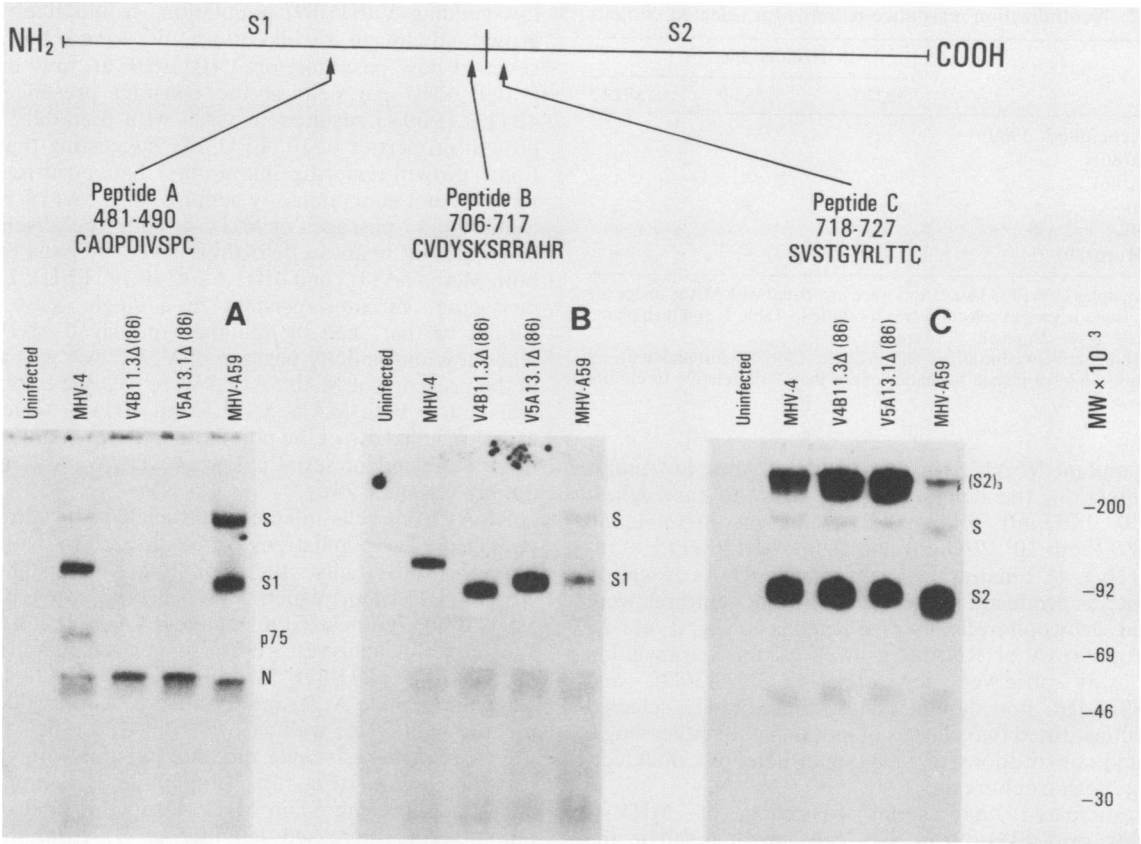


FIG. 3. Localization of the S deletions in 1986 variants to amino acid sequences present in the middle of the amino-terminal S1 fragment by Western blot analysis. Virions harvested from Sac- cultures were solubilized by heating to 100°C for 5 min, and proteins were separated on Tris-bicine slab gels before electrophoretic transfer to nitrocellulose sheets. Immobilized proteins were then incubated in the presence of rabbit antipeptide antibodies A, B, and C, directed against the indicated portions of the MHV A59 S protein. After a second incubation with $^{125}$I-labeled protein A, the sheets were rinsed, air dried, and exposed to Kodak XAR film.

the original neutralization-resistant variants selected in 1986 were deletion mutants. Indeed, examination of 1988 MHV-4 stocks, prepared after three 1-day passages of the 1986 MHV-4 population in Sac- culture, revealed that deletion mutants were present in proportions high enough to be detected as a minor RNA 3 species in Northern blot analyses (data not shown). This finding suggested that once formed, deletion mutants are selectively amplified in Sac- culture, but it did not provide information regarding the frequency of their formation.

To determine whether deletions are frequently generated, we first isolated MHV-4 from the 1986 stock by repeated plaque purification, and a 1989 stock was prepared by three 1-day amplifications of the virus obtained from a single plaque. Because the deletion mutants V5A13.1Δ(86) and V4B11.3Δ(86) were known to be equally resistant to both MAbs 4B11.6 and 5A13.5 (7), we next subjected the 1989 stock to both of these MAbs, singly and in combination. As controls, the earlier 1986 stock as well as the 1988 stock known by Northern analysis to contain high proportions of deletion mutants were tested.

The results of the neutralization tests (Table 1) indicated that the passaged 1986 and 1988 stocks contained variants resistant to both MAbs at frequencies of $10^{-3}$ and $10^{-1}$, respectively. In contrast, variants resistant to both MAbs were not present among $2 \times 10^5$ PFU of the replaqued 1989 stock (Table 1). Instead, infectivity remained only when MAbs were used singly. These two newly selected variant populations, termed V4B11(89) and V5A13(89), were selected from the replaqued 1989 stock at frequencies of $3 \times 10^{-5}$, well below the variant frequencies present in the earlier-passaged stocks.

After three rounds of neutralization, we characterized these newly selected populations by first analyzing their patterns of resistance to neutralizing S-specific MAbs. Unlike the deletion mutants, these 1989 variants displayed resistance only to the MAb used to select them (Table 2). Second, the relative growth rates of the single-MAb-resistant variants were compared with wild-type MHV-4 and

TABLE 1. Frequencies of MAb-resistant variants in MHV stocks[a]

| MHV-4 stock | % PFU resistant to selecting MAb | | |
|---|---|---|---|
| | 4B11.6 | 5A13.5 | 4B11.6 + 5A13.5 |
| 1986 | 0.24 | 0.45 | 0.11 |
| 1988 | 12 | 20 | 13 |
| Replaqued, 1989 | 0.0027 | 0.0027 | <0.00045 |

[a] Virus stocks were mixed with an equal volume of a 1:10 dilution of MAb ascites fluid and incubated for 1 h at 22°C. Serial dilutions were prepared by using 1:20 dilutions of MAb and seeded on DBT cell monolayers. MAbs (1:50) were present in the overlay medium during the 3-day plaque development period.

TABLE 2. Neutralization resistance patterns for selected variants

| Virus[a] | Neutralization by[b]: | | |
|---|---|---|---|
| | 4B11.6 | 5A13.5 | 5B19.3 |
| MHV-4 (replaqued, 1989) | + | + | + |
| V4B11.3Δ(86) | − | − | + |
| V5A13.1Δ(86) | − | − | + |
| V4B11(89) | − | + | + |
| V5A13(89) | + | − | + |
| V5A13/4B11Δ(89) | − | − | + |

[a] Virus samples (100 PFU in 0.25 ml) were incubated with MAbs under the conditions used for variant selection (see footnote to Table 1) and then plated on DBT cells for development of plaques.

[b] +, MAb effectively neutralized all infectivity (>99% neutralization); −, MAb did not diminish plaque formation more than 30% relative to control values.

deletion mutant V5A13.1 in Sac- culture. After low-multiplicity infection, the deletion mutant grew to the highest yields ($10^6$ PFU/ml), followed by wild type MHV-4 and V5A13(89) (both $10^5$ PFU/ml) and then V4B11(89) ($5 \times 10^2$ PFU/ml) (Fig. 4). Finally, the virus-specific RNAs as well as the S proteins produced in these infected Sac- cultures were compared electrophoretically (see legends to Fig. 1 and 2). Coelectrophoresis of RNA 3 as well as its S translation product was observed for MHV-4, V5A13(89), and V4B11(89) (data not shown). Thus, these newly selected variants constituted two classes of mutants with either single amino acid substitutions or very small deletions undetectable by gel electrophoresis.

We anticipated that serial passaging of MHV-4, V5A13(89), or V4B11(89) in Sac- cells might result in the regeneration and amplification of rare viable S1 deletion mutants. Such a mutation, particularly if it occurred in the low-yielding V4B11(89) population, would likely confer a growth advantage in cell culture. We found, however, that seven 1-day passages of V4B11(89) at low multiplicity (<0.01 PFU per cell) in the constant presence of MAb 4B11.6 (1:50×) resulted in virus with markedly improved growth properties (>$10^5$ PFU/ml), suggesting that an additional growth-restoring mutation(s) had occurred, but the virus did not concomitantly acquire MAb 5A13.5 resistance. Similarly, 15 passages of MHV-4(89) in the absence of any MAb did not result in detectable levels of virus resistant to both MAbs 5A13.5 and 4B11.6 (<1 in $10^6$ PFU). During this passaging, variants resistant to a single MAb remained similar to that seen in minimally passaged MHV-4. Only when low multiplicity passage of V5A13(89) was performed in the presence of MAb 5A13.5 were we able to obtain virus resistant to both MAbs 5A13.5 and 4B11.6, which by passage 7 reached 5% of the population. Thus, in only one of the three independent serial passages were we able to select a doubly resistant virus.

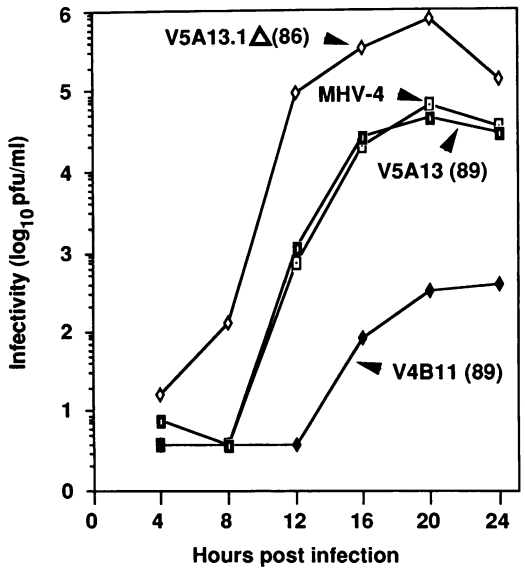


FIG. 4. Time course of MHV-4 and variant virus production in Sac- cell culture. Cells were distributed into 35-mm-diameter tissue culture wells and allowed to grow to confluence ($2 \times 10^6$ cells per well) before inoculation with the indicated viruses at 0.005 PFU per cell. After virus absorption, unattached inoculum was removed and 2 ml of medium was added to each well. At the indicated times after infection, cells were scraped into medium, and the resulting suspensions were frozen at −70°C. Infectivity in the clarified freeze-thaw extracts was determined by titration on DBT indicator cells.

RNAs from cells infected with each of the three serially passaged virus populations were analyzed by Northern blot hybridization. Only the double-MAb-resistant variant V5A13/4B11Δ(89), which was selected after passage of V5A13(89), synthesized a smaller RNA 3 (data not shown). Western blot analyses were also performed on the virion proteins of V4B11(89), V5A13(89), and V5A13/4B11Δ(89), using antipeptide A, B, and C antisera. Antipeptide A serum reacted with S1 as well as p75 from wild-type MHV-4 and the two single-resistance mutants but not with the doubly resistant mutant (Fig. 5). Antipeptide B serum identified coelectrophoresing S1 in MHV-4 and the single-resistance mutants; the increased mobility of S1 from the double-resistance mutant was consistent with a 15-kDa deletion in this chain. Antipeptide C serum bound to coelectrophoresing S2 cleavage products from all virions; trimers of S2 were also seen in three of the four preparations. These analyses reinforced the contention that virus resistant to only one MAb contained point mutants, whereas virus resistant to both MAbs contained at least one deletion in S1 whose size and location was similar to that seen in the original 1986 mutants.

**Variants with deletions in S are selectively amplified only in cell lines sensitive to virus-induced cell fusion.** In four of six murine cell lines, we found MHV-4 to be highly cytopathic, with virus-induced cell fusion ultimately resulting in destruction of the cultures. These fusion-sensitive cultures included DBT and Sac-, two lines generally used for propagation of virus, as well as C1300 and Neuro 2A, two peripheral neuroblastoma cell lines. All of the deletion mutants, although cytopathic, exhibited a delayed induction of fusion in these four cell lines. By microscopic examination, this was most evident in the DBT cell line. After inoculation at high multiplicity, cell fusion reached 30% by 6 h postinfection in wild-type-infected cultures, whereas a similar degree of fusion was not observed until 12 h postinfection in parallel V5A13/4B11Δ(89)-infected cells (Fig. 6). Even after 24 h, when detached syncytia were all that remained in MHV-4-infected cultures, variant infection failed to recruit about half of DBT cells into syncytia (Fig. 6, bottom panels).

Direct assays of viral titers produced in these fusion-sensitive cell lines showed that delayed cytotoxicity was correlated with higher yields. In DBT and Sac-, the output titers of deletion variants V4B11.3Δ(86) and V5A13.1Δ(86) were 10 to 100 times higher than titers of wild-type MHV-4; in C1300 and Neuro 2A, the yields of deletion mutants were similarly 5- to 10-fold higher than yields of wild-type virus

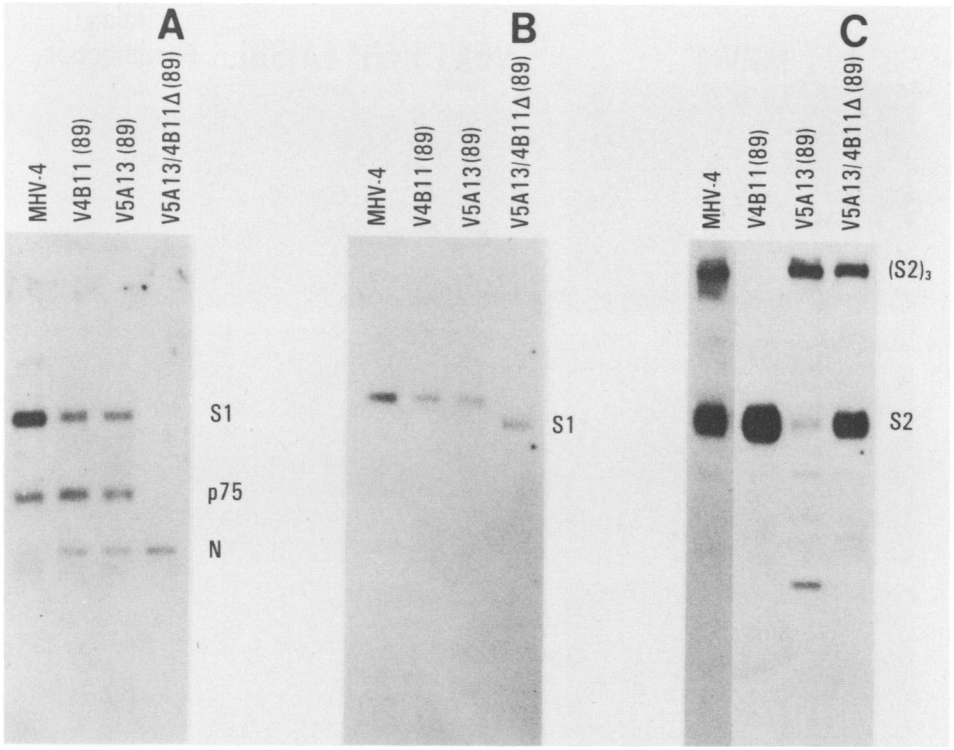


FIG. 5. Characterization of newly isolated (1989) variants by Western blotting. Virion proteins were probed with antipeptide antibodies A, B, and C (panels A, B, and C, respectively) as described in the legend to Fig. 3. Before analysis, the viruses were passaged three times [MHV-4 and V5A13(89)] or five times [V4B11(89)] in Sac- cells. V5A13/4B11Δ(89) was selected from V5A13(89) at passage 7 and then amplified twice before virion purification.

(Table 3). Essentially identical results were obtained with the reselected V5A13/4B11Δ(89) deletion mutant (data not shown).

In contrast to the fusion-sensitive lines, two neuroblastomas derived from murine olfactory bulb, lines OBL 21 and OBL 21A, produced progeny virus in the absence of cytopathic effect or cell fusion. These two cultures produced similar but low yields of both wild-type and deletion mutant virus (Table 3). In addition, murine brains inoculated intracerebrally consistently produced more wild-type virus (Table 3). Together with the observations made for the fusing cell lines, these results suggest that the deletion mutants do not have an inherent ability to produce more progeny but rather that their reduced cytotoxicity simply allows cells to survive long enough for continuation of virion RNA, protein, and progeny PFU production.

This hypothesis was tested by monitoring the rate of virus-specific RNA synthesis in DBT (fusion-sensitive) and OBL 21A (fusion-resistant) cells infected with either wild-type or variant MHV. Such measurements are relatively straightforward because coronavirus mRNA synthesis is not blocked by dactinomycin, an inhibitor of DNA-directed RNA synthesis (27). Thus, the incorporation of [$^3$H]uridine into acid-insoluble material after dactinomycin treatment is indicative of viral RNA synthesis rates.

Incorporation studies showed that in the first 10 h of DBT infection, the kinetics of RNA synthesis were nearly identical for the two viruses; from 10 to 28 h postinfection, however, variant RNA synthesis continued, whereas wild-type RNA synthesis rapidly declined (Fig. 7A). Viral RNA synthesis in MHV-4-infected DBT cultures was no longer detectable by 14 h postinfection; however, variant-specific RNA synthesis was observed even after 28 h. This RNA synthesis profile correlated well with the differential rate and extent of cell destruction in the two infections (Fig. 6). In addition, the time course was consistent with the observation of 100-fold-higher variant virus yields at 24 h postinfection (Table 3). Infectivity of MHV is known to decline rapidly at 37°C in medium at neutral pH (32). Thus, both the decreased overall production of MHV-4 and the longer period of progeny virus inactivation occurring between the end of the growth cycle and the time of virus harvest contributed to the lower yields of MHV-4.

In contrast to the DBT cells, daily monitoring of MHV-4 and variant RNA synthesis rates in OBL 21A cells revealed similar incorporation in the two cultures at 1 day postinfection (Fig. 7B). This result was consistent with the similar yields of the two virus types in this line (Table 3). The higher rates of MHV-4 RNA synthesis at days 2, 3, and 4 (Fig. 7B) may reflect a slight preference for the replication of this virus during long-term OBL 21A infection.

## DISCUSSION

In this report, we have demonstrated selection of MHV-4 populations containing various alterations in the S peplomer. Two types of heterogeneity were observed. First, putative point mutants were isolated. These variants represent the expected outcome of neutralizing MAb pressure on the RNA virus population. Second and more striking was the observation of deletion mutants lacking about 400 nucleotides in the middle portion of S fragment S1. The size of these deletions is remarkably similar to that of previously identified S-deletion mutants (26, 35); determination of whether

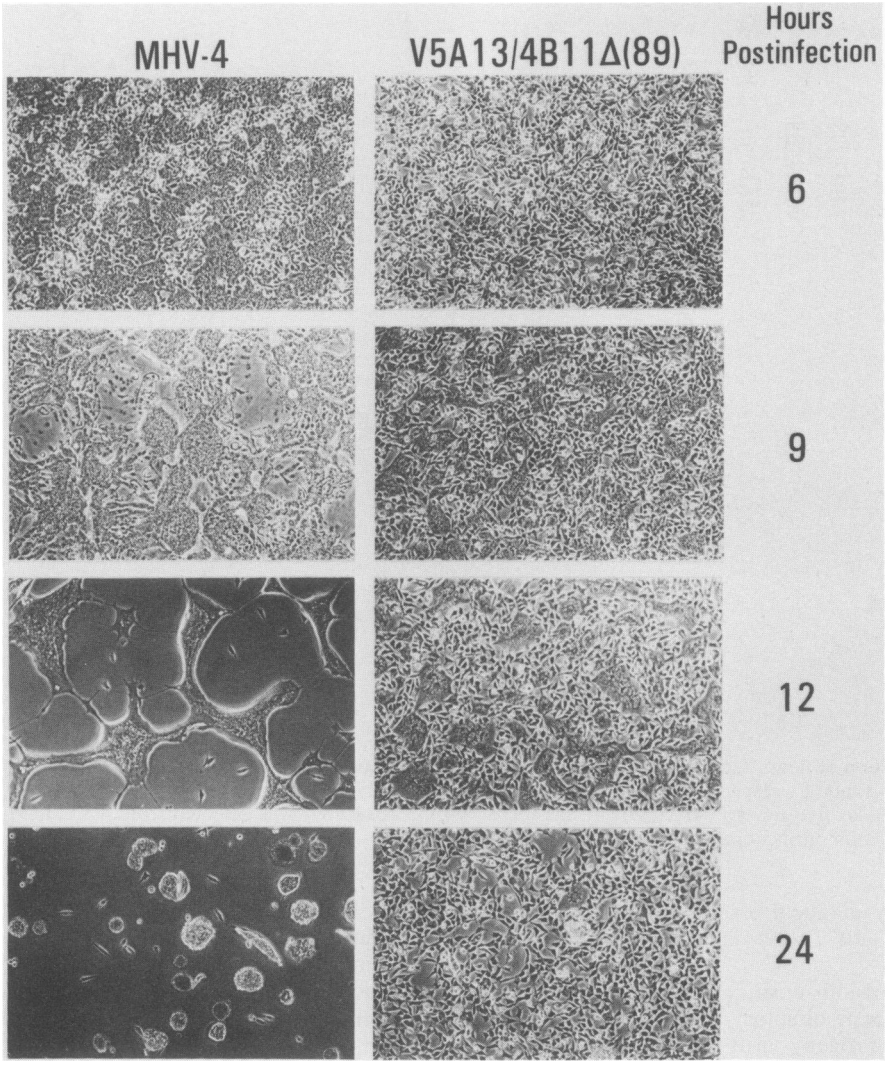


FIG. 6. Illustration of cytopathic effects produced by MHV-4 and variant V5A13/4B11Δ(89). DBT cells ($2 \times 10^5/cm^2$) were inoculated at 2 PFU per cell and photographed at the indicated times postinfection with a Nikon Diaphot phase-contrast microscope. Magnification, ×200.

these other deletions also map to the S1 fragment awaits further studies.

**Deletion mutations arise at lower frequencies than putative point mutations.** These two types of S heterogeneity are best explained by high- and low-frequency errors made during RNA polymerization. Substitution error frequencies of $10^{-4}$ per base after a limited number of replications are commonly observed in viral RNA polymerases (30). This high frequency of error is similar to our observed frequency of putative point mutants in minimally passaged stocks. Errors giving rise to deletion mutants may arise by a copy choice (also referred to as jumping polymerase) mechanism similar to that proposed for the generation of defective interfering (DI) RNAs in many viruses (18). A similar scenario has been proposed for the generation of recombinants in cells coinfected with two different strains of MHV (17). In this hypothetical scheme, a complex of RNA polymerase and nascent genome is transferred from one template position to another at homologous or nonhomologous sites. Replication reinitiation and elongation direct the completion of a defective RNA or, in the case of MHV, viable deletion mutant or true recombinant RNA genomes.

DI RNAs of MHV have been observed after multiple passaging of virus stocks or after establishment of persistent infection (22). As with DI virus generation, we could generate viable deletion mutants only after serial passaging; even then, only one of three passages resulted in deletion selection. Thus, deletion mutation within the S open reading frame is less frequent than point mutation and is very rare relative to the previously reported 10% frequencies of RNA recombination between closely related MHV strains (23). Possibly this is because the transfer of RNA polymerase and nascent genome from its original site to a downstream site on the template does not involve RNA base pairing, unlike the event giving rise to true recombinants. Indeed, we have not found homology between various deletion endpoints by direct RNA sequencing (26a). In addition, low frequencies may result because the only permitted deletion mutations are those that do not compromise virus viability; frameshifts or omissions of essential sequence information would result in defective RNA genomes. Thus, these viable deletion mutants likely arise at frequencies at least as low as those of their nonviable counterparts, the DI RNAs.

**Selective forces determine the size of the S gene of MHV-4.**

TABLE 3. Yields of wild-type and deletion mutant viruses in selected neuronal and nonneuronal cell cultures and in murine brain

| Host | Fusion[a] | Virus yields[b] | | |
|---|---|---|---|---|
| | | Wild-type MHV-4 | V4B11.3Δ(86) | V5A13.1Δ(86) |
| DBT[c] | + | 2.2 | 208 | 188 |
| SAC− | + | 320 | 3,000 | 2,800 |
| C1300 | + | 192 | 1,280 | 800 |
| Neuro 2A | + | 148 | 1,760 | 1,480 |
| OBL 21 | − | 1.6 | 0.6 | 1.2 |
| OBL 21A | − | 2.2 | 1.3 | 1.0 |
| BALB/c brain[d] | | | | |
| 2 days | | 380 | 140 | ND |
| 4 days | | 57 | 14 | 2 |

[a] +, Synctium formation in MHV-infected cells; −, no synctium formation.
[b] Values for cell cultures are expressed as PFU × $10^{-4}$ per milliliter; values for BALB/c brain tissue are expressed as PFU × $10^{-3}$ per gram. ND, Not determined.
[c] Adherent cell monolayers ($10^5$ cells per $cm^2$) were inoculated at 0.01 PFU per cell. After 24 h at 37°C, virus released into each culture was titered by plaque assay on DBT cells.
[d] Samples of 0.05 ml containing $10^3$ PFU were inoculated intracerebrally into 6-week-old mice (three mice per datum point). After the indicated incubation periods, brains were removed and homogenized, and virus infectivity in the resultant 10% (wt/vol) suspensions was determined on DBT cells.

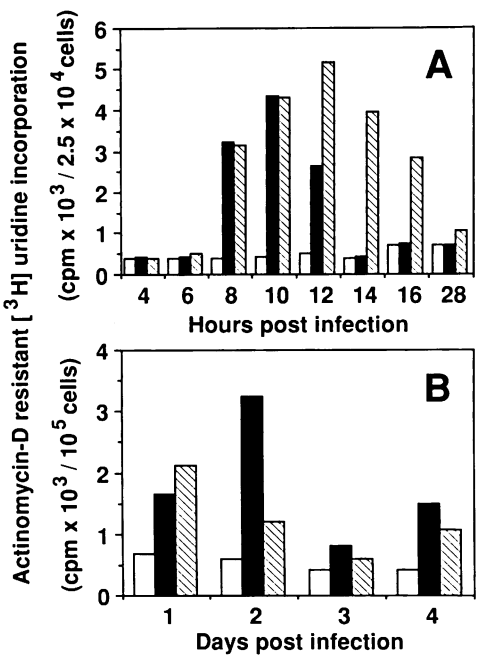


FIG. 7. Time courses of viral RNA synthesis in DBT (A) and OBL 21A (B) cells infected with wild-type MHV-4 and deletion mutant V5A13/4B11Δ(89) (2 PFU per cell). Identical monolayers of uninfected (□), MHV-4-infected (■), and V5A13/4B11Δ(89)-infected (▨) cells were incubated at 37°C in complete growth medium; 1 h before the indicated times, cells were treated with medium containing 5 μg of dactinomycin per ml. Pulse-labeling was initiated 0.5 h later by replacement with medium containing dactinomycin and 5,6-[$^3$H]uridine (0.01 mCi/ml). After a 0.5-h (DBT cells) or 2-h (OBL 21A cells) labeling period, the acid-insoluble radioactivity present in the adhered cell monolayer was determined by liquid scintillation spectroscopy.

Although the frequency of viable deletion mutants is clearly very low, we have found that these mutants nonetheless eventually amplify greatly in cell culture because of their ability to yield more progeny than does wild-type virus. This result clearly indicates that a 15-kDa domain in S fragment S1 is dispensable for in vitro virus growth and that its presence actually limits virus growth in some but not all cell cultures. However, our finding that the replication of deletion mutants in the murine brain is poor relative to that of wild-type virus suggests that this portion of S1 provides useful in vivo functions and that it would be maintained through serial in vivo passages. In this regard, it is notable that Taguchi et al. (36) isolated variants of MHV JHM from the brains of Lewis rats that contained S apoproteins 15 kDa larger than that seen in the virus stock used for inoculation. One likely explanation for this result is that predominantly deletion mutant inoculum was used and that selective replication of a minor component containing MHV-4-sized S occurred in the rat brain. In a separate study by Morris et al. (26), virus was isolated from the spinal cord of persistently infected Wistar-Furth rats that harbored an S smaller than the inoculum used. Taken together, these results suggest that the host strain or the central nervous system location (brain or cord) may control S size selection in vivo.

**Decreased cytopathic properties are a common feature of deletion mutants.** All of our deletion mutants displayed a relatively weak cytopathic effect and a longer growth cycle, permitting higher yields of progeny virus than of wild-type virus. In addition, all of the mutants were significantly neuroattenuated when inoculated intracerebrally into BALB/c mice (7; T. Gallagher, unpublished observations). These characteristics are strikingly similar to those previously described for MHV JHM variants isolated from persistently infected Sac- (2) and DBT (12) cells. Our finding that infection of DBT cells with an S-deletion mutant leaves a high proportion of infected survivors (Fig. 6 and 7) suggests that persistently infected cells may select for viruses lacking this dispensable S1 domain. Clearly, one possibility that remains to be explored concerns the relative abundance of deletion mutants in the few cells surviving an acute MHV-4 infection.

The correlation between the length and productivity of the MHV growth cycle and the degree of cytopathology was further reinforced by our finding that the two central nervous system neuronal lines, OBL 21 and 21A, which were resistant to the cytopathic effects of S, supported both wild-type and deletion mutant viruses with equal but low efficiency. Thus, it appears that one primary factor limiting the production of MHV-4 in vitro is its propensity to kill fusion-sensitive cells before extensive virion formation occurs. At present, we know that MHV-4 synthesizes as much viral RNA and S protein as do the deletion mutants at the early stages of infection (Fig. 2 and 7). In addition, preliminary pulse-chase analyses indicate that wild-type and mutant S proteins are transported intracellularly and incorporated into virions with identical kinetics. Therefore, we favor the hypothesis that omission of sequences in the S1 fragment results in a decrease in the specific fusogenicity of the S molecule.

**Point mutants will be useful for the precise identification of neutralizing epitopes.** All available evidence supports the contention that our newly selected 1989 variants contain substitution mutations conferring resistance to neutralizing MAbs. Thus, the nucleotide sequence of these variant S genes, which is currently being determined, will no doubt provide a more precise identification of the epitopes defined by MAbs 4B11.6 and 5A13.5. At present, only one site

involved in neutralization has been mapped on the S sequence of MHV (20). This MAb-binding site was conserved among all MHV strains. In contrast, the MAb 4B11.6 and 5A13.5 epitopes are found only on highly virulent strains of MHV (37). Detailed analysis of these epitopes associated with virulence will contribute to an understanding of coronavirus pathogenesis.

## ACKNOWLEDGMENTS

This work was supported by Public Health Service grants AI 25913 and NS 12428 from the National Institutes of Health. T.M.G. was supported by Public Health Service training grant 5-T32-AG00080 from the National Institutes of Health. S.E.P. was supported by a postdoctoral fellowship from the Multiple Sclerosis Society.

We thank Joseph O'Neill for technical assistance.

## LITERATURE CITED

1. **Bailey, O. T., A. M. Pappenheimer, F. S. Cheever, and J. B. Daniels.** 1949. A murine virus (JHM) causing disseminated encephalomyelitis with extensive destruction of myelin. II. Pathology. J. Exp. Med. **90**:195–212.
2. **Baybutt, H. N., H. Wege, M. J. Carter, and V. ter Meulen.** 1984. Adaptation of coronavirus JHM to persistent infection of murine Sac- cells. J. Gen. Virol. **65**:915–924.
3. **Buchmeier, M. J., P. J. Southern, B. S. Parekh, M. K. Wooddell, and M. B. A. Oldstone.** 1987. Site-specific antibodies define a cleavage site conserved among arenavirus GP-C glycoproteins. J. Virol. **61**:982–985.
4. **Burnette, W. N.** 1981. Western blotting: electrophoretic transfer of proteins from sodium dodecyl sulfate-polyacrylamide gels to unmodified nitrocellulose and radiographic detection with antibody and radioiodinated protein A. Anal. Biochem. **112**:195–203.
5. **Cavanaugh, D.** 1983. Coronavirus IBV: structural characterization of the spike protein. J. Gen. Virol. **64**:2577–2583.
6. **Collins, A. R., R. L. Knobler, H. Powell, and M. J. Buchmeier.** 1982. Monoclonal antibodies to murine hepatitis virus-4 (strain JHM) define the viral glycoprotein responsible for attachment and cell-cell fusion. Virology **119**:358–371.
7. **Dalziel, R. G., P. W. Lampert, P. J. Talbot, and M. J. Buchmeier.** 1986. Site-specific alteration of murine hepatitis virus type 4 peplomer glycoprotein E2 results in reduced neurovirulence. J. Virol. **59**:463–471.
8. **Fleming, J. O., S. A. Stohlman, R. C. Harmon, M. M. C. Lai, J. A. Frelinger, and L. P. Weiner.** 1983. Antigenic relationships of murine coronaviruses: analysis using monoclonal antibodies to JHM (MHV-4). Virology. **131**:296–307.
9. **Fleming, J. O., M. D. Trousdale, F. A. K. El-Zaatari, S. A. Stohlman, and L. P. Weiner.** 1986. Pathogenicity of antigenic variants of murine coronavirus JHM selected with monoclonal antibodies. J. Virol. **58**:869–875.
10. **Frana, M. F., J. N. Behnke, L. S. Sturman, and K. V. Holmes.** 1985. Proteolytic cleavage of the E2 glycoprotein of murine coronavirus: host-dependent differences in proteolytic cleavage and cell fusion. J. Virol. **56**:912–920.
11. **Haspel, M. V., P. W. Lampert, and M. B. A. Oldstone.** 1978. Temperature-sensitive mutants of mouse hepatitis produce a high incidence of demyelination. Proc. Natl. Acad. Sci. USA **75**:4033–4036.
12. **Hirano, N., N. Goto, S. Makino, and K. Fujiwara.** 1981. Persistent infection with mouse hepatitis virus JHM strain in DBT cell culture, p. 301–308. *In* V. ter Meulen, S. Siddell, and H. Wege (ed.), Biochemistry and biology of coronaviruses. Plenum Publishing Corp., New York.
13. **Johnson, D. A., J. W. Gautsch, J. R. Sportsman, and J. H. Elder.** 1984. Improved technique utilizing nonfat dry milk for analysis of proteins and nucleic acids transferred to nitrocellulose. Gene Anal. Techn. **1**:3–8.
14. **Johnstone, A., and R. Thorpe.** 1982. Immunochemistry in practice. Blackwell Scientific Publications, Ltd., Oxford.
15. **Kessler, S. W.** 1975. Rapid isolation of antigens from cells with a staphylococcal protein A-antibody adsorbent: parameters of the interaction of antibody-antigen complexes with protein A. J. Immunol. **115**:1617–1624.
16. **Knobler, R. L., L. A. Tunison, P. W. Lampert, and M. B. A. Oldstone.** 1982. Selected mutants of mouse hepatitis virus type 4 (JHM strain) induce different CNS diseases. Am. J. Pathol. **109**:157–165.
17. **Lai, M. M. C., S. Makino, L. H. Soe, C.-K. Shieh, J. G. Keck, and J. O. Fleming.** 1987. Coronaviruses: a jumping RNA transcription. Cold Spring Harbor Symp. Quant. Biol. **52**:359–365.
18. **Lazzarini, R. A., J. D. Keene, and M. Schubert.** 1981. The origins of defective interfering particles of the negative strand RNA viruses. Cell **26**:145–154.
19. **Lehrach, H., D. Diamond, J. M. Wozney, and H. Boedtker.** 1977. RNA molecular weight determinations by gel electrophoresis under denaturing conditions, a critical reexamination. Biochemistry **16**:4743–4751.
20. **Luytjes, W., Geerts, D., W. Posthumus, R. Meloen, and W. Spaan.** 1989. Amino acid sequence of a conserved neutralizing epitope of murine coronaviruses. J. Virol. **63**:1408–1412.
21. **Luytjes, W., L. S. Sturman, P. J. Bredenbeek, J. Charite, B. A. M. van der Zeijst, M. C. Horzinek, and W. J. M. Spaan.** 1987. Primary structure of the glycoprotein E2 of coronavirus MHV-A59 and identification of the trypsin cleavage site. Virology **161**:479–487.
22. **Makino, S., N. Fujioka, and K. Fujiwara.** 1985. Structure of the intracellular defective viral RNAs of defective interfering particles of mouse hepatitis virus. J. Virol. **54**:329–336.
23. **Makino, S., J. G. Keck, S. A. Stohlman, and M. M. C. Lai.** 1986. High frequency RNA recombination of murine coronaviruses. J. Virol. **57**:729–737.
24. **Maniatis, T., E. F. Fritsch, and J. Sambrook.** 1982. Molecular cloning: a laboratory manual. Cold Spring Harbor Laboratory, Cold Spring Harbor, N.Y.
25. **Melton, D. A., P. A. Krieg, M. R. Rebagliati, T. Maniatas, K. Zinn, and M. R. Green.** 1984. Efficient in vitro synthesis of biologically active RNA and RNA hybridization probes from plasmids containing a bacteriophage SP6 promoter. Nucleic Acids Res. **12**:7035–7056.
26. **Morris, V. L., C. Tieszer, J. Mackinnon, and D. Percy.** 1989. Characterization of coronavirus JHM variants isolated from Wistar Furth rats with a viral-induced demyelinating disease. Virology **169**:127–136.

26a. **Parker, S. E., T. M. Gallagher, and M. J. Buchmeier.** 1989. Sequence analysis reveals extensive polymorphism and evidence of deletions within the E2 glycoprotein gene of several strains of murine hepatitis virus. Virology **173**:664–673.

27. **Robb, J. A., and C. W. Bond.** 1979. Coronaviridae, p. 193–247. *In* H. Frankel-Conrat and R. R. Wagner (ed.), Comprehensive virology, vol. 14. Plenum Publishing Corp., New York.
28. **Schmidt, I., M. Skinner, and S. Siddell.** 1987. Nucleotide sequence of the gene encoding the surface projection glycoprotein of coronavirus MHV-JHM. J. Gen. Virol. **68**:47–56.
29. **Spaan, W., D. Cavanagh, and M. C. Horzinek.** 1988. Coronaviruses: structure and genome expression. J. Gen. Virol. **69**: 2939–2952.
30. **Steinhauer, D. A., and J. J. Holland.** 1987. Rapid evolution of RNA viruses. Annu. Rev. Microbiol. **41**:409–433.
31. **Stohlman, S., P. Brayton, J. Fleming, L. Weiner, and M. Lai.** 1982. Murine coronaviruses: isolation and characterization of two plaque morphology variants of JHM neurotropic strain. J. Gen. Virol. **63**:265–275.
32. **Sturman, L. S.** 1981. The structure and behavior of coronavirus A59 glycoproteins, p. 1–18. *In* V. ter Meulen, S. Siddell, and H. Wege (ed.), Biochemistry and biology of coronaviruses. Plenum Publishing Corp., New York.
33. **Sturman, L. S., K. V. Holmes, and J. Behnke.** 1980. Isolation of coronavirus envelope glycoproteins and interaction with the viral nucleocapsid. J. Virol. **33**:449–462.
34. **Sturman, L. S., C. S. Ricard, and K. V. Holmes.** 1985. Proteolytic cleavage of the E2 glycoprotein of murine coronavirus:

activation of cell-fusing activity of virions by trypsin and separation of two different 90K cleavage fragments. J. Virol. **56**:904–911.

35. **Taguchi, F., and J. O. Fleming.** 1989. Comparison of six different murine coronavirus JHM variants by monoclonal antibodies against the E2 glycoprotein. Virology **169**:233–235.
36. **Taguchi, F., S. G. Siddell, H. Wege, and V. ter Meulen.** 1985. Characterization of a variant virus selected in rat brains after infection by coronavirus mouse hepatitis virus JHM. J. Virol. **54**:429–435.
37. **Talbot, P. J., and M. J. Buchmeier.** 1985. Antigenic variation among murine coronaviruses: evidence for polymorphism on the peplomer glycoprotein, E2. Virus Res. **2**:317–328.
38. **Talbot, P. J., A. A. Salmi, R. L. Knobler, and M. J. Buchmeier.** 1984. Topographical mapping of epitopes on the glycoproteins of murine hepatitis virus-4 (strain JHM): correlation with biological activities. Virology **132**:250–260.
39. **Wege, H., R. Dorries, and H. Wege.** 1984. Hybridoma antibodies to the murine coronavirus JHM: characterization of epitopes on the peplomer protein (E2). J. Gen. Virol. **65**:1931–1942.
40. **Wege, H., J. Winter, and R. Meyermann.** 1988. The peplomer protein E2 of coronavirus JHM as a determinant of neurovirulence: definition of critical epitopes by variant analysis. J. Gen. Virol. **69**:87–98.
41. **Weiner, L. P.** 1973. Pathogenesis of demyelination induced by a mouse hepatitis virus (JHM virus). Arch. Neurol. **28**:298–303.